Title

Variability of gas composition and flux intensity in natural marine hydrocarbon seeps

Journal

Geo-Marine Letters: An International Journal of Marine Geology, 30(3)

ISSN

1432-1157

Authors

Clark, Jordan F.
Washburn, Libe
Schwager Emery, Katherine

Publication Date

2010-06-01

DOI

10.1007/s00367-009-0167-1

Peer reviewed

Geo-Mar Lett (2010) 30:379–388
DOI 10.1007/s00367-009-0167-1

ORIGINAL

Variability of gas composition and flux intensity in natural marine hydrocarbon seeps

Jordan F. Clark · Libe Washburn · Katherine Schwager Emery

Received: 13 March 2009 / Accepted: 29 September 2009 / Published online: 17 October 2009

Abstract The relationship between surface bubble composition and gas flux to the atmosphere was examined at five large seeps from the Coal Oil Point seep field (Santa Barbara Channel, CA, USA). The field research was conducted using a flux buoy designed to simultaneously measure the surface bubbling gas flux and the buoy's position with differential GPS, and to collect gas samples. Results show that the flux from the five seeps surveyed a total of 11 times ranged from 800–5,500 m^3 day^{-1}. The spatial distribution of flux from the five seeps was well described by two lognormal distributions fitted to two flux ranges. The seafloor and sea surface composition of bubbles differed, with the seafloor bubbles containing significantly more CO_2 (3–25%) and less air (N_2 and O_2). At the sea surface, the mole fraction of N_2 correlated directly with O_2 ($R^2 = 0.95$) and inversely with CH_4 ($R^2 = 0.97$); the CO_2 content was reduced to the detection limit (<0.1%). These data demonstrate that the bubble composition is modified by gas exchange during ascent: dissolved air enters, and CO_2 and hydrocarbon gases leave the bubbles. The mean surface composition at the five seeps varied with water depth and gas flux, with more CH_4 and higher CH_4/N_2 ratios found in shallower seeps with higher flux. It is suggested that the CH_4/N_2 ratio is a good proxy for total or integrated gas loss from the rising bubbles, although additional study is needed before this ratio can be used quantitatively.

J. F. Clark (✉) · K. Schwager Emery
Department of Earth Science, University of California,
Santa Barbara, CA 93106, USA
e-mail: jfclark@geol.ucsb.edu

L. Washburn · K. Schwager Emery
Department of Geography, University of California,
Santa Barbara, CA 93106, USA

K. Schwager Emery
Department of Ecology, Evolution and Marine Biology,
University of California,
Santa Barbara, CA 93106, USA

Introduction

Natural hydrocarbon seeps are important contributors to the global carbon cycle. They are conduits for the transfer of buried sedimentary carbon, which takes the form of methane (CH_4) and other heavy hydrocarbons including oil, to the atmosphere and ocean. How important marine seeps are to the atmospheric CH_4 cycle is debatable and depends on assumptions about the ability of the ocean to dissolve CH_4 released either as bubbles or pieces of hydrates at the seafloor. The ocean is potentially a significant barrier because it is able to absorb and oxidize these gases in situ (Reeburgh 2003, 2007).

Seafloor vents create plumes of rising bubbles, which have been observed in a variety of environments (for a summary of locations, see Judd and Hovland 2007). Large bubble plumes, such as those observed in the Santa Barbara Channel, modify the environment of the near-field water column (e.g., Leifer et al. 2000). In addition to creating large gradients in dissolved gas concentrations due to bubble–water gas transfer, the rising bubble plumes entrain ambient ocean water and generate upward vertical flows (e.g., McDougal 1978; Schladow 1992; Leifer et al. 2000, 2006; Zhang 2003; Clark et al. 2003). Thus, the upward movement of bubbles results from their own buoyancy and the rising column of plume water. Because the total amount of gas dissolving into the water column depends upon the integrated flux over the bubbles' lifetime, the rise velocity is important. Large bubble plumes that generate strong

vertical flows significantly decrease the transit time from the seafloor to the surface, and thus increase the flux of seep gas to the atmosphere.

The gas exchange rate and direction are determined by the concentration gradient across the bubble–water interface. Carbon dioxide (CO_2), CH_4, and other hydrocarbon gases are transferred out of rising bubbles, while nitrogen (N_2), oxygen (O_2), and other dissolved gases are transferred into the bubbles. Plume processes that affect the amount of gas exchange include plume-water saturation and the generation of upward vertical flows. Limited field observations (e.g., Leifer et al. 2000, 2006) suggest that both of these processes scale with flux. Furthermore, gas exchange rates are dependent on bubble size, and recent observations indicate that bubble size distributions differ above strong and weak seafloor vents (Leifer and Culling 2010, this issue). Strong vents emit a broader bubble spectrum, which includes large bubbles. Model calculations indicate that a smaller fraction of the initial mass dissolves from large bubbles than from small bubbles during transit through the water column (Leifer and MacDonald 2003). Modeling studies also indicate that oil on the bubble walls can slow the rate of gas exchange between the bubbles and plume water.

This paper addresses the relationship between bubbling gas flux to the atmosphere and gas composition using field measurements from the Coal Oil Point seep field. We evaluate the hypothesis that the composition of the bubbles at the sea surface can be used as a proxy for the amount of gas exchange that occurs during the bubbles' transit through the water column. We hypothesized that, due to seep hydrodynamics, bubbles above stronger seeps would contain more hydrocarbon gases (e.g., CH_4) and less air (N_2 and O_2) than would bubbles at weaker seeps. Verification of this hypothesis would imply that (1) compared with seeps with higher flux, a greater fraction of the gas released at the seafloor from seeps with lower flux dissolves into the water column, and (2) large seeps are less efficient at transferring CH_4 and other hydrocarbon gases into the water column, and more efficient at transferring these gases to the atmosphere.

Field site

The Coal Oil Point seeps are a regional source of hydrocarbons to the atmosphere and ocean. The seeps are located in Santa Barbara County, CA, offshore of the University of California, Santa Barbara (Fig. 1), about 10 km west of the city of Santa Barbara. At various locations within this seep field, bubbles are observed to rise through the water column to the surface, creating areas of bursting bubbles at the sea surface. In addition to contributing significant amounts of tar to regional beaches (Del Sontro et al. 2007) and to the seafloor (Farwell et al. 2009), these seeps are known sources of CH_4 and other hydrocarbon gases to the regional air column (Killus and Moore 1991; Hornafius et al. 1999), and of dissolved hydrocarbons to the coastal ocean (Clark et al. 2000; Mau et al. 2007, 2010, this issue). Sonar surveys suggest that the total gas flux to the atmosphere is on the order of 1×10^5 m^3 day^{-1} (Hornafius et al. 1999). Assuming an average composition of 60% CH_4 (see below), the CH_4 flux is approx. 30 mol s^{-1} (1.5×10^{-5} Tg $year^{-1}$). An approximately equal amount of CH_4 dissolves above the seafloor vents (Clark et al. 2000), creating a plume that extends for 10 s to 100 s of km in the Santa Barbara Channel (Clark et al. 2000; Mau et al. 2007) and the Southern California Bight (Cynar and Yayanos 1992).

The Coal Oil Point seep field has been mapped numerous times using visual observations of surface and seafloor features (i.e., bursting bubbles, seafloor vents, etc.), remote sensing, and sonar surveys (Allen et al. 1970; Fischer 1978; Estes et al. 1985; Hornafius et al. 1999; Quigley et al. 1999; Leifer et al. 2004, 2010, this issue; Kinnaman et al. 2010, this issue). These studies have revealed that seepage occurs within an area of approx. 20 km^2 at water depths ranging from about 10–70 m (Fig. 1). At any given time the total area of bursting bubbles at the sea surface is much smaller, and is distributed among distinct regions determined by the seafloor geology (Hornafius et al. 1999; Leifer et al. 2010, this issue). Seep flux, defined as gas volume emitted per area of sea surface at standard pressure and temperature, is highly variable in space and time. Objective mapping of bubbling gas flux using a flux buoy (Washburn et al. 2001) showed that spatial scales over which bubbling gas flux was correlated were typically a few meters, and that areas of strong flux range from a few hundred to several thousand

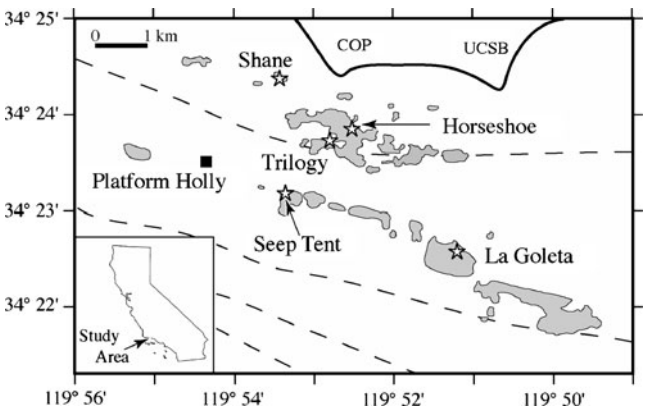

Fig. 1 Map of the Coal Oil Point seep field with the area of active seepage determined during a sonar survey in September 2005 (Leifer et al. 2010, this issue). The *dashed lines* are the 50, 100, 200, and 300 m bathymetric contours. Locations of the five large seeps studied are indicated with *stars*, and the oil production platform, Holly, is indicated with the *square*

m^2 (Washburn et al. 2005). These results are consistent with the sonar and SCUBA survey evidence that many small seafloor vents contribute to the extensive areas of bubbling gas flux at the sea surface.

Other observations from the Coal Oil Point field indicate that seepage rates vary over a broad range of time scales, so that the source functions of CH_4 and other gases are not constant in time (e.g., Quigley et al. 1999; Leifer et al. 2004; Leifer and Boles 2005; Kinnaman et al. 2010, this issue). Temporal variations have been associated with a number of physical processes including surface gravity waves (Leifer and Boles 2005), tides (Boles et al. 2001), and longer-term changes resulting from anthropogenic hydrocarbon production (Quigley et al. 1999). Visual observations of surface bubbles reveal changes in gas flux on time scales of seconds to minutes due to rising "curtains" of bubbles, and possibly flux variability in seafloor vents. At least one large seep, referred to as the Trilogy seep, became active sometime between 1999 and 2005 due to processes that are unclear.

Seeps within the Coal Oil Point field also exhibit a broad range of sizes. The smallest are vents from which small streams of individual bubbles with narrow bubble size distributions emanate. Also commonly found are larger vents, typically crater seeps with diameters of 1 m or less, which form bubble plumes with a broad size distribution. Bubble radii in these plumes range from <500 to >5,000 μm (Leifer et al. 2006; Leifer and Culling 2010, this issue). This type of seep has been found in SCUBA and submersible surveys to form the bubble curtains previously observed near the sea surface. In areas of the seafloor where numerous point and crater seeps are located together, bubble streams combine into single large plumes with high vertical flow velocities and elevated dissolved CH_4 concentrations. The surface expressions of these combined seeps can be easily identified from surveying vessels, and are characterized by large areas of bursting bubbles with corresponding divergent surface flows.

Materials and methods

Seepage flux at the sea surface was determined with the flux buoy, a ~3 m long spar buoy and associated instrumentation that measures gas flux by capturing bubbles just below the sea surface (at ~1.5 m depth). Details of its design, operation, and calibration are given by Egland (2000), Washburn et al. (2001, 2005), and Schwager (2005). The long, narrow configuration of the flux buoy dampens motions due to small-amplitude, high-frequency surface gravity waves, a source of analytical noise. Rising bubbles are directed into a collection chamber through a circular cone (A=0.27 m^2) at the base of the buoy. The flux, q, is determined from the rate of change of the pressure difference, Δp, between the inside of the collection chamber and the surrounding seawater. Gas accumulates in the chamber until an adjustable threshold in Δp is reached. Then a microcomputer-controlled valve opens to release the accumulated gas; this starts a new measurement cycle. Data acquisition, valve operation, and data transmission are controlled by a microcomputer in the electronics pressure case. The computer records Δp, the chamber temperature, T_c, and the chamber pressure, p_c, from which q is estimated once per second. Buoy position is logged every 2 s using a differential global positioning system (GPS) receiver mounted on the top of the spar. In field operations, the buoy is either allowed to drift freely or it is gently towed through seepage areas as the research boat moves slowly forward.

The flux buoy measures the total flux of gas at the sea surface. Compositional analyses are needed to estimate fluxes of individual gases such as CH_4. To measure surface composition, we utilized two approaches. In the one, surface bubbles were collected independently of the flux buoy surveys either using swimmers or directly from the small boats with a funnel and collapsible bag, which was initially filled with seawater. After a collection period, the accumulated gas in the bag was transferred to glass septa bottles, which had previously been purged with helium, using a glass syringe. In the other approach, the flux buoy was modified so that the vented gas could be sampled for later laboratory analysis. Copper tubing (3/8" O.D. and ~2 m length) ran from the submerged collection chamber vent to sample loops, which were located above the water line near the top of the spar. The vented gas was collected in 40-cm-long, 3/8" stainless steel tubes sealed with Nupro plug valves. These tubes were bent into "U-shape" loops so that the outlet end could be placed into a small container of seawater. This created a seal, and prevented air from contaminating the seep gas samples; it also enabled field personnel to see when the accumulated seep gas had vented. After collection, these loops could be quickly replaced from the side of the boat. When operating the flux buoy in the sample collection mode, a helium gas line was attached to the base of the funnel, so that prior to collecting seep gas the funnel, collection chamber, transfer lines, and loops could be flushed. One or two helium blanks were collected during each survey to determine the efficiency of the helium flush.

At three deeper large seeps, La Goleta (65 m depth), Horseshoe (40 m depth), and Trilogy (45 m depth), which could not be sampled with SCUBA divers, seafloor vent gas was collected using the *Delta* submersible during September 2005 (see Fig. 1 for seep locations). Seafloor surveys revealed that these seeps are composed of hundreds of vents that ranged in size from ~0.5 m diameter craters to

small point vents. Both types of vents were sampled using an inverted funnel collection system attached to the outside of the submersible. With this system, the seep gas was collected in 3/8" stainless steel tubes that were sealed with Nupro plug values. Seep gas was transferred from these tubes to glass septa bottles, which had previously been flushed with helium gas, within a few hours after collection on board the R/V *Velero IV*, the support vessel.

In the laboratory, the seep gas in sample loops or septa bottles was removed using a glass syringe. Subsequently, this gas was analyzed with standard methods on an Agilent micro-gas chromatograph (GC) for CH_4, O_2, N_2, and carbon dioxide (CO_2), or a Schimadzu GC for ethane (C_2H_6), propane (C_3H_8), and butane (C_4H_{10}), using (respectively) a thermal conductivity detector (TCD) or flame ionization detector (FID) and helium as the carrier gas. The typical analytical uncertainty of the measurements and collection based on replicates is better than ±3%.

Field cruises

Four of the large seep areas were surveyed with the flux buoy two or more times each between 2002 and 2005 (Table 1). The largest seep area, the Seep Tents, was surveyed only once in 2002. Two additional surveys were conducted away from any visible seepage to characterize the instrument noise, which is generated by swell moving the buoy up and down. Results of these surveys are discussed by Washburn et al. (2005). The buoy was gently pulled through the seep areas usually for about 4 h during the morning before afternoon wind-driven waves developed, as typically happens in the Santa Barbara Channel. The buoy was positioned to maximize the time it remained over areas of bubbles; no predetermined grid pattern was used. As a result, the webs of survey lines were denser near areas of strongest bubbling gas flux, such as at Trilogy seep (Fig. 2). The total flux for each seep area was determined by objectively mapping q onto a 2 m×2 m grid using standard geo-statistical techniques to produce estimates of mean q in each grid square, and then summing the mean q over the survey area (Washburn et al. 2005). Surface currents caused locations of the surface expression of the seeps to change with time, but these occurred slowly over the ~4 h sampling periods, and no corrections were applied.

Composition–flux surveys at two seeps, La Goleta and Seep Tents, were conducted during two survey days (16 December 2003, and 5 October 2004). Each of these seep areas is composed of smaller regions of high flux (hereafter referred to as "sub-seeps") surrounded by broader areas of lower flux. The different sub-seeps are visually distinct, and samples were collected from different areas by carefully positioning the flux buoy in a given sub-seep. This often required steering the boat in small circles. Because surface gas flux varied strongly, the length of time required to fill the collection chamber was as short as 10 s of seconds and as long as a half hour.

Results

Flux and area estimates of bubbling gas flux

The flux buoy surveys within the Coal Oil Point seep field indicate that the areas with measurable levels of q at the sea surface ranged from about 800–5,500 m^2 (16–42 m diameters; Table 1). These areas are identified in Table 1 by names and positions, which does not account for all areas with visible bursting bubbles within the field. Estimates of mean flux averaged over these areas vary from 0.4–5.1 $m^3\ m^{-2}\ day^{-1}$ (or m day^{-1}, as given by Washburn et al. 2005).

Table 1 indicates that the distribution of flux was skewed toward higher values: typically, the highest 5–10% of q measurements for a given seep contributed more than 50% of the total flux q_T (column 7, Table 1). For example, for La Goleta seep on 15 September 2005 about 6% of q samples accounted for 50% of q_T. The cumulative distribution of q interpolated onto the 2 m×2 m grid is shown in Fig. 3. It is derived from 18,973 estimates of q from the five large seeps and the 20-m noise test of Table 1, along with three other smaller seeps not discussed in this paper. Seeps and days included in the cumulative distribution of Fig. 3 are indicated in Table 1. Inclusion of q estimates from the large seeps on different days produced similar results. Measurement noise due to buoy motion caused the cumulative distribution to level out for q less than ~0.03 $m^3\ m^{-2}\ day^{-1}$. For $q \leq 1\ m^3\ m^{-2}\ day^{-1}$, the distribution was well described by the sum of a lognormal distribution and Gaussian noise, as shown by the solid black line of Fig. 3. The lognormal portion was determined from a least square fit over the range $0.04 \leq q < 1\ m^3\ m^{-2}\ day^{-1}$, and parameters for this distribution and the Gaussian noise are indicated in Fig. 3. A lognormal distribution plots as a straight line for the axes of Fig. 3. For $q > 1\ m^3\ m^{-2}\ day^{-1}$, the observed distribution exceeded the modeled distribution. Another lognormal distribution was fitted over the range $1 \leq q < 10\ m^3\ m^{-2}\ day^{-1}$, and well described the distribution of q over this range. About 13% of q values exceeded $1\ m^3\ m^{-2}\ day^{-1}$. For $q > 10\ m^3\ m^{-2}\ day^{-1}$, encompassing about 0.04% of values, the observed distribution departed sharply upward, indicating an excess of a few high fluxes compared to the lognormal distribution. We speculate that this resulted from sampling bias, since measurements were concentrated in areas with the highest flux. It also may have resulted from areas of strong flux at scales smaller than the 2 m×2 m averaging area used to estimate q.

Table 1 Flux buoy survey results (*ST* Seep Tents, *La Gol* La Goleta, *HS* Horseshoe, *Tri* Trilogy, *NT* Noise Test)

Seep (depth)	Location	Survey dates	n[a]	Mean q[b] ($m^3m^{-2}day^{-1}$)	$q_{max.}$[c] ($m^3m^{-2}day^{-1}$)	q_T[d] (m^3day^{-1})	A (m^2)	% contributing to 50% of q_T[e]
HS (40 m)	34°23.757′, 119° 52.530′	6 Dec. 02	14,407	0.9	10.9	2,392	2,710	6.4
HS (40 m)	34°23.757′, 119° 52.530′	13 Dec. 02	12,933	0.7	5.4	3,653	5,274	6.5
HS (40 m)[f]	34°23.757′, 119° 52.530′	17 Jan. 03	12,736	1.5	11.5	3,372	2,253	6.8
La Gol (65 m)	34°22.523′, 119° 51.258′	29 Aug. 02	8,169	1.0	7.1	1,249	1,266	7.4
La Gol (65 m)[f]	34°22.523′, 119° 51.258′	20 Jun. 03	13,356	1.7	8.1	800	480	4.3
La Gol (65 m)	34°22.523′, 119° 51.258′	15 Sep. 05	13,292	0.4	6.2	787	2,113	5.9
ST (67 m)[f]	34°22.523′, 119° 51.258′	22 Nov. 02	15,529	5.1	24	5,732	1,131	9.4
Shane (22 m)[f]	34°23.070′, 119° 53.370′	15 Aug. 02	3,064	3.3	12.4	1,099	331	3.8
Shane (22 m)	34°24.363′, 119° 53.423′	23 Aug. 02	13,216	3.9	24	2,566	666	12.1
Tri (45 m)	34°23.620′, 119° 52.739′	19 Sep. 05	16,364	1.0	8.2	5,472	5,380	9.3
Tri (45 m)[f]	34°23.620′, 119° 52.739′	20 Sep. 05	10,056	0.8	7.6	4,159	5,018	10.1
NT (20 m)[f]	34°24.125′, 119° 52.995′	19 Sep. 02	7,191	–	1.6	−35[g]	–	–
NT (60 m)	34° 22.950′, 119° 53.076′	19 Sep. 02	6917	–	1.2	+15[g]	–	–

[a] Because the sampling rate was 1 sample s^{-1}, the number of samples (minus 1) is also the sampling time in seconds

[b] Mean $q = q_T/A$

[c] The maximum 1-s flux measured during each survey

[d] Total flux calculated by summing the gridded mean flux (see text for details)

[e] Upper percentile of flux measurements needed to reach 50% of q_T (see text for details)

[f] Used in cumulative distribution of Fig. 3

[g] Difference in spatial integrals over positive and negative values of q caused by buoy motion

Repeat surveys at the seeps with high flux showed variability in q_T and A from survey to survey (Table 1), such as at Trilogy seep on 19 and 20 September 2005 as shown in Fig. 2a and b, respectively. The rectangular areas of Fig. 2 are of the same size and centered on the same point (34°23.620′N, 119°52.739′W). The spatial patterns of q during the surveys were very similar, both showing a spatial trend of increasing q toward the western and southern portions of the survey area. The eastward shift by ~20 m of the flux pattern compared with the first survey was likely due to a change in surface currents. q_T, A, maximum flux $q_{max.}$ differed, by 7%, 22%, and 8%, respectively (Table 1). For other seeps, the changes between repeat surveys were larger. For example, during three surveys on 6 and 13 December 2002 and 17 January 2003 at Horseshoe seep, A varied by about 200%, q_T by about 50%, and $q_{max.}$ by about 200%. The largest variation was found at Shane seep during surveys conducted on 15 and 23 August 2002, but this likely resulted from under-sampling. High winds and sea state on 15 August resulted in a shorter survey with few observations of q. This likely accounts for the lower values of mean q and smaller estimated area.

Bubble gas composition

Clark et al. (2003) reported observations of the change in bubble gas composition between the sea surface and seafloor at Shane seep where samples could be collected using SCUBA divers. During this study, seafloor samples were collected at three deeper seeps using the *Delta* submersible, and no mid-water column samples were collected. The O_2 and N_2 fractions of these seafloor samples were unexpectedly high, often greater than 3% and 12%, respectively. A likely source of these gases was air contamination during collection. Therefore, the compositions of the deep seafloor samples have been corrected using the N_2/O_2 ratio of air, and assuming the seep gas

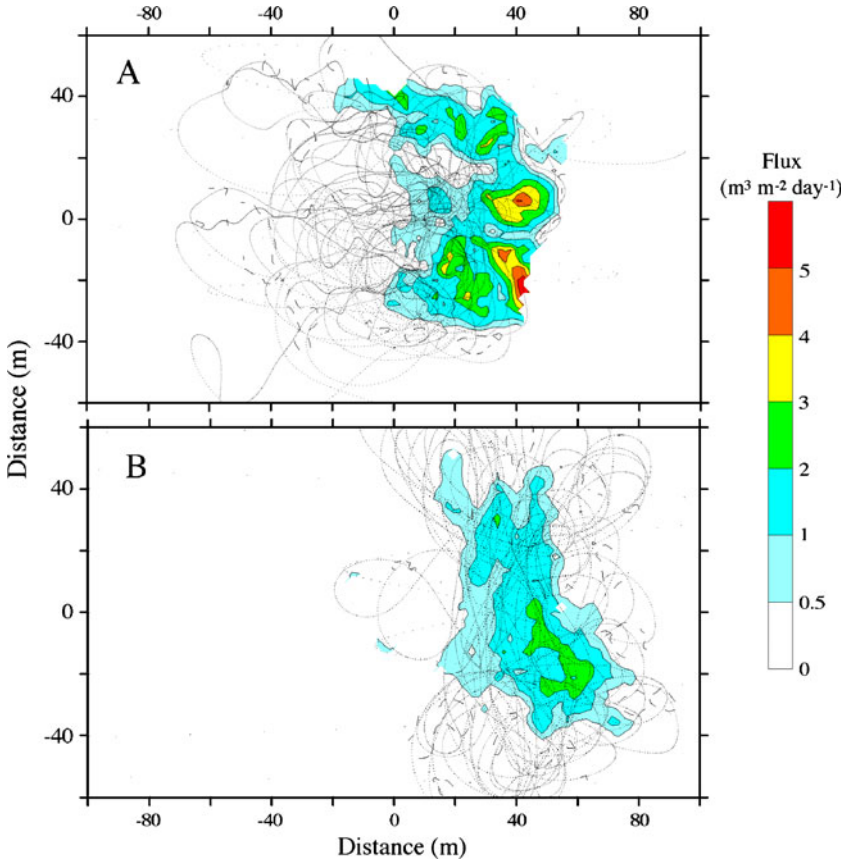

Fig. 2 Contours of the bubbling gas flux, q, at Trilogy seep collected on (**a**) 19 September 2005, and (**b**) 20 September 2005 with the flux buoy. The *gray lines* of measurement points show the survey paths, and north is toward the top. The maps origin is at 34°23.620′N, 119°52.739′W

contained a similar amount of O_2 as Shane seep (0.3%). The corrected compositions of the deeper seeps are similar to the inshore shallow Shane seep, although they are more variable (Table 2). CO_2 and CH_4 together make up approx. 92%, non-methane hydrocarbons (NMHC) ~7%, and nitrogen less than 1%. The two major gas components correlate strongly (R^2 = 0.94), and show that the mole fraction of these gases varies by about 20% (Fig. 4). Each

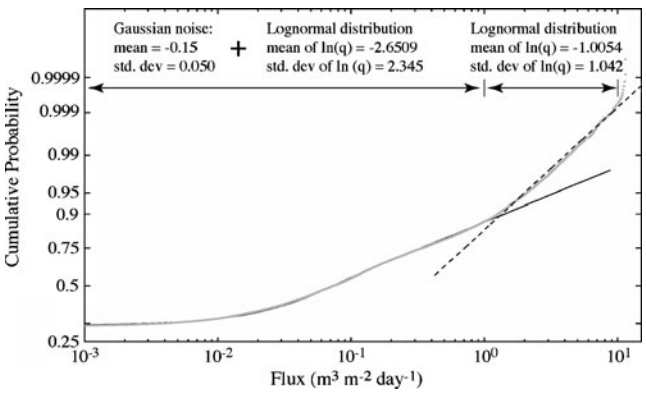

Fig. 3 Cumulative distribution of bubbling gas flux q measured by the seep buoy (*gray dots*). The *solid black line* is the sum of a lognormal distribution fitted over the range $0.04 \le q < 1$ m^3 m^{-2} day^{-1} and Gaussian noise. The *dashed black line* is a lognormal distribution fitted over the range $1 \le q < 10$ m^3 m^{-2} day^{-1}. Means, standard deviations, and fit ranges are indicated at the top of the figure

seep's variability, however, is smaller than the variability over the entire field. The high-CO_2 seeps, Horseshoe and Trilogy, occur at intermediate depths (~50 m) and tend to emit more oil. The Trilogy sample that contained ~25% carbon dioxide was from a vent with low bubbling gas flux, and may reflect local biogeochemical alteration.

Relative to the seafloor samples, the surface gas contains less CO_2 and CH_4, and more N_2 and O_2 (Table 2). The relative abundance of these gases correlated strongly (N_2 vs. CH_4, R^2 = 0.97; O_2 vs. CH_4, R^2 = 0.98; N_2 vs. O_2, R^2 = 0.95). The N_2/O_2 ratios of the seep gas (2.4–3.3) were between the value of air (3.7) and air-saturated water (1.8). This indicates that the bubbles were stripping gas from seawater in which 25–45% of the O_2 had been consumed.

The compositions of surface samples collected with the modified flux buoy were similar to the surface samples collected by hand (Fig. 5), though they tended to contain less air and more CH_4. It is likely that samples collected by hand may have been contaminated slightly with air during collection, though no correction was applied. The modified flux buoy samples were collected within areas of high q from the various sub-seeps over a period of 2–4 h. The high variability of gas composition (10–15%), as quantified by the mole fractions of CH_4 and N_2, indicates large changes over spatial scales of a few to several meters. This variability is similar to the high variability in q on

Table 2 Bubble composition (mole fraction) from large seeps within the Coal Oil Point seep field[a]

Seep	Date	Depth	Flux	N_2	O_2	CH_4	CO_2	NMHC	CH_4/N_2
ST	16 Dec. 03	Surface	1.1	17.7	3.3	71.9	<0.1	7.2	4.07
ST	16 Dec. 03	Surface	1.9	22.2	4.0	67.3	<0.1	6.6	3.04
ST	16 Dec. 03	Surface	3.1	23.6	4.4	65.6	<0.1	6.4	2.79
ST	16 Dec. 03	Surface	1.0	24.9	4.6	64.4	<0.1	6.2	2.59
ST	16 Dec. 03	Surface	1.2	25.2	4.6	64.1	<0.1	6.1	2.54
ST	16 Dec. 03	Surface	0.1	18.6	3.4	70.9	<0.1	7.1	3.81
ST	16 Dec. 03	Surface	0.2	16.3	3.1	73.5	<0.1	7.1	4.50
ST	4 Oct. 04	Surface	–	22.9	4.5	66.2	<0.1	6.5	2.89
ST	4 Oct. 04	Surface	3.9	19.4	3.9	69.8	<0.1	6.9	3.60
ST	4 Oct. 04	Surface	0.1	16.8	3.2	72.6	<0.1	7.4	4.33
ST	4 Oct. 04	Surface	−0.1	22.8	4.5	66.2	<0.1	6.5	2.90
La Gol	4 Oct. 04	Surface	1.0	22.8	4.2	67.4	<0.1	5.6	2.95
La Gol	4 Oct. 04	Surface	1.2	25.3	4.7	64.9	<0.1	5.8	2.56
La Gol	4 Oct. 04	Surface	0.2	19.7	3.7	71.4	<0.1	5.2	3.63
La Gol	4 Oct. 04	Surface	0.1	27.2	4.6	62.6	<0.1	5.6	2.30
Blank	16 Dec. 03	Surface	nd	1.5	0.3	<0.1	<0.1	<0.1	<0.1
Blank	4 Oct. 04	Surface	nd	0.1	0.4	0.2	0.1	<0.1	3.00
HS	20 Sep. 05	Surface	nd	34.3	9.3	50.9	<0.1	5.5	5.50
HS	20 Sep. 05	Surface	nd	37.7	9.6	46.3	<0.1	6.2	4.80
La Gol	20 Sep. 05	Surface	nd	41.3	9.6	45.5	<0.1	3.5	1.10
La Gol	20 Sep. 05	Surface	nd	38.5	9.0	48.6	<0.1	3.8	1.26
La Gol	20 Sep. 05	Surface	nd	39.8	9.3	47.3	<0.1	3.7	1.19
Tri	20 Sep. 05	Surface	nd	27.5	7.2	59.4	0.1	5.8	2.16
Tri	20 Sep. 05	Surface	nd	33.6	8.3	52.4	<0.1	5.7	1.56
Tri	20 Sep. 05	Surface	nd	30.4	7.9	55.9	<0.1	5.7	1.84
HS	20 Sep. 05	Seafloor	nd	4.3	0.3	72.3	15.3	7.7	16.8
HS	20 Sep. 05	Seafloor	nd	5.1	0.3	75.9	10.9	7.2	14.9
HS	20 Sep. 05	Seafloor	nd	3.1	0.3	75.0	13.6	8.0	24.2
HS	20 Sep. 05	Seafloor	nd	1.2	0.3	77.8	12.3	8.7	64.8
La Gol	16 Sep. 05	Seafloor	nd	3.8	0.3	76.6	12.8	6.5	20.2
La Gol	19 Sep. 05	Seafloor	nd	2.2	0.3	81.9	10.1	5.7	37.2
La Gol	16 Sep. 05	Seafloor	nd	2.1	0.3	89.7	3.1	4.9	42.7
La Gol	19 Sep. 05	Seafloor	nd	3.4	0.3	83.4	6.2	6.9	24.5
Tri	17 Sep. 05	Seafloor	nd	2.5	0.3	64.0	25.5	7.8	25.6
Tri	17 Sep. 05	Seafloor	nd	4.4	0.3	70.7	16.3	7.9	16.1

[a] The seafloor samples were corrected for air contamination using the method described in the text. ST, Seep Tents; La Gol, La Goleta; HS, Horseshoe; Tri, Trilogy; nd, not determined

comparable spatial scales. However, the fraction of CH_4 at these seeps did not correlate with q (Fig. 6), indicating that the amount of gas exchange is not a simple function of bubbling gas flux within the seep area.

Discussion and summary

Detailed mapping of bubbling gas flux q and bubble composition at large seeps from the Coal Oil Point seep field show high variability over spatial scales of a few meters. Repeat surveys separated by days to years (Table 1) show that total flux q_T, seep area A, and maximum flux $q_{max.}$ were highly variable. We speculate that these differences are due to changes in gas emission rates from the seafloor, since sampling was very dense in areas of strongest seepage, which dominate estimates of q_T. Additionally, data could be collected only during similar, calm sea states. The magnitude of change in q_T is much larger than variability caused by tides, a likely environmental parameter that could cause these differences. For example, Boles et al. (2001) analyzed time series of q_T at the nearby Seep Tents (65 m depth, adjacent to the Seep Tents seep), and found that variability due to tides was less than 7%. The observed distribution for q in the range $0.04 \leq q < 10$ m^3 m^{-2} day^{-1}, accounting for 56% of samples, was well

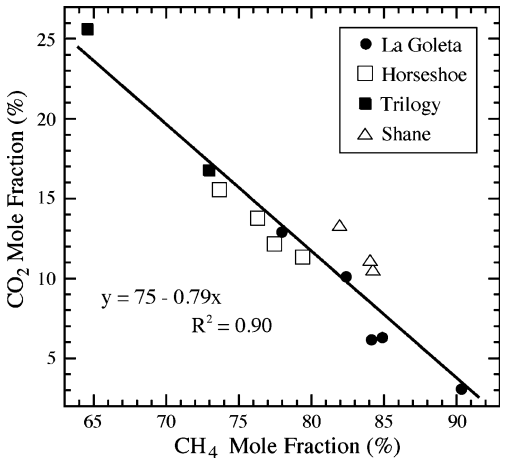

Fig. 4 Composition of the CH_4 and CO_2 at the seafloor. Symbols in the legend indicate sampling locations. Samples from Horseshoe (40 m water depth), Trilogy (45 m), and La Goleta (65 m) seeps were collected from the *Delta* submersible; samples from Shane seep were collected by SCUBA divers and are from Clark et al. (2003)

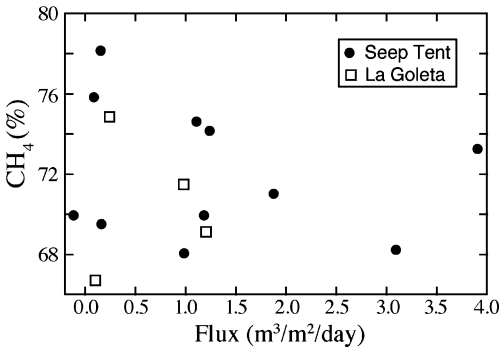

Fig. 6 CH_4 mole fraction versus bubbling gas flux q from Seep Tents and La Goleta seeps collected using the flux buoy

described by two lognormal distributions fitted over two flux ranges. The distribution was not well resolved for lower q values, due to instrument noise, and for higher values due to over-sampling of high-flux regions or inadequate spatial resolution of flux estimates. The total flux from the five seeps surveyed ranges between 15×10^3 and 19×10^3 m^3 day^{-1}, 15–19% of the estimated total flux from the Coal Oil Point seep field.

Comprehensive observations of the change in bubble gas composition between the sea surface and seafloor have been made at the relatively shallow but intense (mean q of 3–4 m^3 m^{-2} day^{-1}; Table 1) Shane seep (Clark et al. 2003).

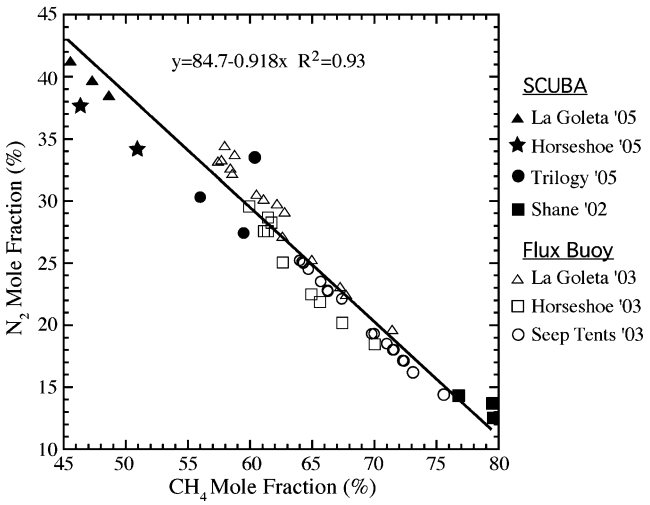

Fig. 5 Mole fractions of N_2 and CH_4 measured by SCUBA divers and the modified flux buoy. Symbols in the legend indicate sampling locations and collection methods. The Shane seep data are from Clark et al. (2003)

Because of its shallow depth (~22 m), the fieldwork could be conducted easily with SCUBA divers. In addition to collecting bubble samples, divers were able to map seafloor features in detail (Leifer et al. 2004, 2006). Bubbles 1 m above the seafloor vents were composed primarily of CH_4 (83%), CO_2 (12%), and NMHC (non-methane hydrocarbons, 2.9%); components of air, including N_2 and O_2, contributed less than 2% of the total volume (Clark et al. 2003). The presence of O_2 indicates that some gas exchange occurred below the 1 m height of the sampling point, possibly within the sediments. Shallow circulation cells commonly form in sediments near seeps (O'Hara et al. 1995; Zimmermann et al. 1997), and could be the source of this O_2. At shallower depths the CO_2 mole fraction decreased to the analytical detection limit, whereas the air fraction increased. At the surface, bubbles were composed of CH_4 (78%), N_2 (14%), O_2 (5.3%), and NMHC (2.4%). The mole fractions of CH_4 and NMHC reached maxima at mid-depths due to the more rapid loss of CO_2 relative to the inflow of air (Clark et al. 2003).

With the exception of Shane seep, repeat surveys of bubble composition were not conducted (Clark et al. 2003). Given the large range of compositions determined during the flux buoy surveys of the sub-seeps, which were sampled over a period of a few hours, it is likely that the temporal variability would not exceed the spatial variability. While the mole fractions of the major gases (CH_4, N_2, and O_2) correlated strongly ($R^2 > 0.95$), gas composition at the surface did not correlate with bubbling gas flux within the seeps (Fig. 6). This implies that gas exchange between the bubbles and ambient water is not a simple function of gas flux. Several factors may account for this, including (1) chaotic local circulation patterns of large bubble plumes, which may cause bubble–plume water separation and entrainment of ambient ocean water; (2) variations in the seafloor composition of vent gas; (3) variations in the bubble size distributions; and (4) variations in the gas exchange rate caused by differing amounts of surfactants (i.e., oil) coating the bubbles.

Evidence from vertical profiles of bubble composition at Shane seep shows that CO_2 is rapidly lost from the rising bubbles, presumably due to chemically enhanced gas transfer (e.g., Emerson 1975). Analyses of gas collected from the Seep Tents approx. 10 m above the seafloor and piped to shore (Clark et al. 2000) are consistent with these observations of rapid CO_2 loss. When CO_2 is excluded, the re-normalized mole fractions of the vent gas components are similar, being 89.5±4.2% and 3.3±1.5% for CH_4 and N_2, respectively. Because gas compositions are reported as mole fractions (rather than concentrations), the loss or gain of one component affects the mole fractions of the other components. This effect is seen in the vertical profile of bubble composition above Shane seep. Because of the rapid loss of CO_2, the CH_4 mole fraction is at a maximum at mid-depths (Clark et al. 2003). Therefore, the best way to assess the amount of gas exchange is to look at the relative change in gases, such as CH_4 and N_2, which are being lost and gained from the rising bubbles. As gases exchange, the CH_4/N_2 ratio will decrease from the seafloor value of about 30, to about 0 at the surface. The latter is reached when all of the CH_4 has been lost from the bubble. It is possible for a bubble plume to reach the sea surface and emit no CH_4 to the atmosphere. This would occur if all of the CH_4 had been replaced by air stripped from the water column.

Seep field trends of gas transfer can be inferred from the CH_4 and N_2 data using mean compositions. Because only five large seeps were examined, the trends are more qualitative than quantitative. The highest CH_4 and CH_4/N_2 ratios were found at the surface of Seep Tents and Shane seeps, the two most intense seeps (i.e., highest mean q and $q_{max.}$, see Table 1). The shallower of these two seeps (Shane) contained higher values of CH_4 and CH_4/N_2 ratios. La Goleta seep, which has a similar depth as Seep Tents, contained less CH_4 and had a lower CH_4/N_2 ratio; it is a much weaker seep. Similar to the Seep Tents–La Goleta trend discussed above, Horseshoe, which has a similar depth to Trilogy but lower total flux, had less CH_4 and a lower CH_4/N_2 ratio. The amount of gas exchange, and therefore CH_4 loss, scales directly with depth and inversely with seepage intensity. Because of the small sample size (n=5), it is not possible to quantify these relationships. To establish the CH_4/N_2 ratios as a proxy for total gas exchange between the seafloor and surface, additional work is needed. Most importantly, model simulations are needed. Nevertheless, these limited field data support our hypothesis that large seeps emit a larger fraction of their CH_4 and other hydrocarbon gases to the atmosphere than do small seeps.

The detailed mapping of the surface expression of five large Coal Oil Point seeps reveals that their seepage intensity and gas composition vary over short temporal and spatial scales. Seafloor surveys indicate that some of the surface variability is inherited from below; seafloor seeps are distributed over a broad area, and consist of both point vents and larger craters that emit curtains of bubbles. The variation in bubble composition, however, suggests that bubble plume dynamics also contributes to the surface variability by influencing the bubble–water gas transfer rate. Finally, the repeat flux buoy investigations show intra-survey differences in A and q_T indicating that sedimentary processes that control the vent emission rates must also contribute to the temporal variability.

Acknowledgements This study was supported by the University of California Energy Institute and the West Coast NURP program under ward No. NA03OAR4300104, subcontract UAF-05-0140 from the National Oceanic and Atmospheric Administration (NOAA), U.S. Department of Commerce. The fieldwork was conducted with the help of Shane Anderson, David Farrar, and David Salazar. The gas analyses were conducted in the laboratory of Dr. David Valentine at UCSB with the assistance of Dr. Frank Kinnaman. The manuscript benefited from the careful reviews of Dr. Erwin Suess and an anonymous reviewer. Thanks also to the crew of the R/V *Velero* and the *Delta* submarine. The statements, findings, conclusions, and recommendations are those of the authors and do not necessarily reflect the views of NOAA, the Department of Commerce, or the University of California, Santa Barbara.

References

Allen AA, Schlueter RS, Mikolaj PG (1970) Natural oil seepage at coal oil point, Santa Barbara, California. Science 170:974–977

Boles JR, Clark JF, Leifer I, Washburn L (2001) Temporal variation in natural methane seep rate due to tides, Coal Oil Point area, California. J Geophys Res 106:27,077–27,086

Clark JF, Washburn L, Hornafius JS, Luyendyk BP (2000) Dissolved hydrocarbon flux from natural marine seeps to the southern California Bight. J Geophys Res 105:11,509–11,522

Clark JF, Leifer I, Washburn L, Luyendyk BP (2003) Compositional changes in natural gas bubble plumes: observations from the Coal Oil Point marine hydrocarbon seep field. In: Woodside JM, Garrison RE, Moore JC, Kvenvolden KA (eds) Proc 7th Int Conf Gas in Marine Sediments, 7–12 October 2002, Baku, Azerbaijan. Geo-Mar Lett SI 23(3/4):187–193. doi:10.1007/s00367-003-0137-y

Cynar FJ, Yayanos AA (1992) The distribution of methane in the upper waters of the Southern California Bight. J Geophys Res 97:11,269–11,285

Del Sontro TS, Leifer I, Luyendyk BP, Broitman BR (2007) Beach tar accumulation, transport mechanisms, and sources of variability at Coal Oil Point, California. Mar Pollut Bull 54:1461–1471

Egland ET (2000) Direct capture of gaseous emissions from natural marine hydrocarbon seeps offshore of Coal Oil Point, Santa Barbara, California. MSc Thesis, University of California, Santa Barbara, CA

Emerson S (1975) Chemically enhanced CO_2 gas exchange in a eutrophic lake: a general model. Limnol Oceanogr 20:743–753

Estes JE, Crippen RE, Star JL (1985) Natural oil seep detection in the Santa Barbara Channel, California, with shuttle imaging radar. Geology 13:282–284

Farwell C, Reddy CW, Peacock E, Nelson RK, Washburn L, Valentine DL (2009) Weathering and the fallout plume of heavy oil from strong petroleum seeps near Coal Oil Point, CA. Environ Sci Technol 43:3542–3548

Fischer PJ (1978) Oil and tar seeps, Santa Barbara basin, California. In: California offshore gas, oil, and tar seeps, California State Lands Commission, Sacramento, CA, pp 1–62

Hornafius JS, Quigley D, Luyendyk BP (1999) The world's most spectacular marine hydrocarbon seeps (Coal Oil Point, Santa Barbara Channel, California): quantification of emissions. J Geophys Res 104:20,703–20,711

Judd A, Hovland M (2007) Seabed fluid flow. Cambridge University Press, New York

Killus JP, Moore GE (1991) Factor analysis of hydrocarbon species in the south-central coast air basin. J Appl Meteorol 30:733–743

Kinnaman FS, Kimball J, Busso L, Birgel D, Ding H, Hinrichs K-U, Valentine DL (2010) Gas flux and carbonate occurrence at a shallow seep of thermogenic natural gas. In: Bohrmann G, Jørgensen BB (eds) Proc 9th Int Conf Gas in Marine Sediments, 15–19 September 2008, Bremen. Geo-Mar Lett SI 30 (in press)

Leifer I, Boles JR (2005) Turbine tent measurements of marine hydrocarbon seeps on subhourly timescales. J Geophys Res 110: C01006. doi:10.1029/2003JC002207

Leifer I, Culling D (2010) Bubbles from marine hydrocarbon seepage in the Coal Oil Point seep field. In: Bohrmann G, Jørgensen BB (eds) Proc 9th Int Conf Gas in Marine Sediments, 15–19 September 2008, Bremen. Geo-Mar Lett SI 30 (in press)

Leifer I, MacDonald I (2003) Dynamics of the gas flux from shallow gas hydrate deposits: interaction between oily hydrate bubbles and the ocean environment. Earth Panetary Sci Lett 210:411–424

Leifer I, Clark JF, Chen RF (2000) Modifications of the local environment by natural marine hydrocarbon seeps. Geophys Res Lett 27:3711–3714

Leifer I, Boles JR, Luyendyk BP, Clark JF (2004) Transient discharges from marine hydrocarbon seeps: spatial and temporal variability. Environ Geol 46:1038–1052

Leifer I, Luyendyk BP, Boles JR, Clark JF (2006) Natural marine seepage blowout: contribution to atmospheric methane. Global Biogeochem Cycles 20, GB3008. doi:10.1029/2005GB002668

Leifer I, Kamerling MJ, Luyendyk BP, Wilson DS (2010) Geologic control of natural marine seep hydrocarbon emissions, Coal Oil Point seep field, California. In: Bohrmann G, Jørgensen BB (eds) Proc 9th Int Conf Gas in Marine Sediments, 15–19 September 2008, Bremen. Geo-Mar Lett SI 30 (in press)

Mau S, Valentine DL, Clark JF, Reed J, Camilli R, Washburn L (2007) Dissolved methane distributions and air-sea flux in the plume of a massive seep field, Coal Oil Point, California. Geophys Res Lett 34:L22603. doi:10.1029/2007GL031344

Mau S, Heintz MB, Kinnaman FS, Valentine DL (2010) Compositional variability and air-sea flux of ethane and propane in the plume of a large, marine seep field near Coal Oil Point, CA. In: Bohrmann G, Jørgensen BB (eds) Proc 9th Int Conf Gas in Marine Sediments, 15–19 September 2008, Bremen. Geo-Mar Lett SI 30 (in press)

McDougal TJ (1978) Bubble plumes in stratified environments. J Fluid Mech 4:655–672

O'Hara SCM, Dando PR, Schuster U, Bennis A, Boyle JD, Chui FTW, Hatherell TVJ, Niven SJ, Taylor LJ (1995) Gas seep induced interstitial circulation: observations and environmental implicates. Cont Shelf Res 15:931–948

Quigley DC, Hornafius JS, Luyendyk BP, Francis RD, Clark J, Washburn L (1999) Decrease in natural marine hydrocarbon seepage near Coal Oil Point, California, associated with offshore oil production. Geology 27:1047–1050

Reeburgh WS (2003) Global methane biogeochemistry. In: Keeling R (ed) Treatise on Geochemistry, vol 4. The Atmosphere. Elsevier, Oxford, pp 65–69

Reeburgh WS (2007) Oceanic methane biogeochemistry. Chem Rev 107:486–513

Schladow SG (1992) Bubble plume dynamics in a stratified medium and the implications for water-quality amelioration in lakes. Water Resources Res 28:313–321

Schwager K (2005) Surface gas flux and chemical composition of marine hydrocarbon seeps at Coal Oil Point, California. MSc Thesis, University of California, Santa Barbara, CA

Washburn L, Johnson CG, Gotschalk CC, Egland ET (2001) A gas-capture buoy for measuring bubbling gas flux in oceans and lakes. J Atmos Ocean Technol 18:1411–1420

Washburn L, Clark JF, Kyriakidis P (2005) The spatial scales, distribution, and intensity of natural marine hydrocarbon seeps near Coal Oil Point, California. Mar Petrol Geol 22:569–578

Zhang Y (2003) Methane escape from gas hydrate systems in marine environment and methane-driven oceanic eruptions. Geophys Res Lett 30:1398. doi:10.1029/2002GL016658

Zimmermann S, Hughes RG, Flügel HJ (1997) The effect of methane seepage on the spatial distribution of oxygen and dissolved sulphide within a muddy sediment. Mar Geol 137:149–157